molecular pharmaceutics

articles

Cell Uptake and *in Vitro* Toxicity of Magnetic Nanoparticles Suitable for Drug Delivery

Urs O. Häfeli,*,† Judy S. Riffle,‡ Linda Harris-Shekhawat,‡ Anita Carmichael-Baranauskas,‡ Framin Mark,† James P. Dailey,§ and David Bardenstein||

Faculty of Pharmaceutical Sciences, University of British Columbia, 2146 East Mall, Vancouver, BC V6T 1Z3, Canada, Macromolecules and Interfaces Institute, Virginia Polytechnic Institute and State University, Blacksburg, Virginia 24061, Division of Ophthalmology, Hamot Medical Center, 222 Superior Avenue, Erie, Pennsylvania 16505, and University Hospitals of Cleveland, 11100 Euclid Avenue, Cleveland, Ohio 44106

Received March 17, 2009; Revised Manuscript Received May 11, 2009; Accepted May 15, 2009

Abstract: Magnetic targeting is useful for intravascular or intracavitary drug delivery, including tumor chemotherapy or intraocular antiangiogenic therapy. For all such *in vivo* applications, the magnetic drug carrier must be biocompatible and nontoxic. In this work, we investigated the toxic properties of magnetic nanoparticles coated with polyethylenoxide (PEO) triblock copolymers. Such coatings prevent the aggregation of magnetic nanoparticles and guarantee consistent magnetic and nonmagnetic flow properties. It was found that the PEO tail block length inversely correlates with toxicity. The nanoparticles with the shortest 0.75 kDa PEO tails were the most toxic, while particles coated with the 15 kDa PEO tail block copolymers were the least toxic. Toxicity responses of the tested prostate cancer cell lines (PC3 and C4-2), human umbilical vein endothelial cells (HUVECs), and human retinal pigment epithelial cells (HRPEs) were similar. Furthermore, all cell types took up the coated magnetic nanoparticles. It is concluded that magnetite nanoparticles coated with triblock copolymers containing PEO tail lengths of above 2 kDa are biocompatible and appropriate for *in vivo* application.

Keywords: Toxicity; confocal microscopy; MTT assay; retinal pigment epithelial cells; magnetic nanoparticles; phagocytosis; polyethylene glycole (PEG); polyethylene oxide (PEO)

Introduction

Magnetic particles have two primary uses in medicine: the diagnosis and the treatment of diseases. Established examples of diagnostic applications include the use of ultrasmall superparamagnetic iron oxides (USPIO's) and their multifunctionalized brethren as magnetic resonance imaging (MRI) contrast agents to differentiate metastatic from inflammatory lymph nodes, to give information about tumor angiogenesis, to identify dangerous atherosclerosis plaques,[1−5] and to follow stem cell therapy and transgene expression *in vivo*.[6−8] Therapeutic applications include the magnetic guidance of drugs encapsulated by magnetic particles to target tissues (e.g., a tumor) where they are retained for a controlled treatment period.[9] Such magnetic drug delivery has the key advantage that it allows very concentrated drug doses to be delivered to a target tissue while minimizing the exposure of healthy tissues to the side effects from highly toxic drugs (e.g., chemotherapeutic agents).

* Corresponding author. Tel: (604) 822-7133. Fax: (604) 822-3035. E-mail: uhafeli@interchange.ubc.ca.

† University of British Columbia.

‡ Virginia Polytechnic Institute and State University.

§ Hamot Medical Center.

|| University Hospitals of Cleveland.

(1) Wang, Y. X.; Hussain, S. M.; Krestin, G. P. Superparamagnetic iron oxide contrast agents: physicochemical characteristics and applications in MR imaging. *Eur. Radiol.* **2001**, *11*, 2319–23131.

(2) Tiefenauer, L. X. Chapter 29: Magnetic Nanoparticles As Contrast Agents for Medical Diagnosis In *Nanotechnology in Biology and Medicine: Methods, Devices, and Applications*; Vo-Dinh, T., Eds.; CRC Press, Taylor and Francis: Boca Raton, FL, 2007; pp 1−20.

10.1021/mp900083m CCC: $40.75
Published on Web 05/15/2009

Many different tissues have been studied as potential magnetic drug delivery targets. Delivering drug filled magnetic particles to distinct areas in the liver was most successful,[10−12] but it was also possible to magnetically increase the particles' concentration in the lungs,[13−15] vessel walls,[16] brain,[17,18] and tumors.[19−21] The delivery of magnetic particles to the eye has also been reported and is of interest to the authors.[22−25] Specifically, we plan to use magnetic forces to deliver highly effective but toxic drugs to the back of the eye for the treatment of diseases. Potent drugs for targeted ocular therapy include antiangiogenic agents (e.g., vascular endothelial growth factor (VEGF) inhibitors) for the treatment of exudative age-related macular degeneration (AMD), steroids (e.g., triamcinolone) for the treatment of chronic ocular inflammatory diseases, and anticancer agents for the treatment of intraocular tumors. In addition, magnetically guided transfection has been introduced in recent years[26−30] and might make feasible the treatment of blindness-inducing genetically linked diseases such as retinitis pigmentosa or retinoschisis.

Magnetic particles useful for magnetic drug targeting must be much smaller than red blood cells so that they do not clog the blood capillaries, must be hydrophilic to prevent

(3) Mulder, W. J.; Griffioen, A. W.; Strijkers, G. J.; Cormode, D. P.; Nicolay, K.; Fayad, Z. A. Magnetic and fluorescent nanoparticles for multimodality imaging. *Nanomed.* **2007**, *2*, 307–24.

(4) Morana, G.; Salviato, E.; Guarise, A. Contrast agents for hepatic MRI. *Cancer Imaging* **2007**, *7 Spec No A*, S24–7.

(5) Andrä, W.; Nowak, H. *Magnetism in Medicine: A Handbook*, 2nd ed.; Wiley-VCH Verlag: Weinheim, Germany, 2007.

(6) Lewin, M.; Carlesso, N.; Tung, C. H.; Tang, X. W.; Cory, D.; Scadden, D. T.; Weissleder, R. Tat peptide-derivatized magnetic nanoparticles allow in vivo tracking and recovery of progenitor cells. *Nat. Biotechnol.* **2000**, *18*, 410–414.

(7) Kraitchman, D. L.; Gilson, W. D.; Lorenz, C. H. Stem cell therapy: MRI guidance and monitoring. *J. Magn. Reson. Imaging* **2008**, *27*, 299–310.

(8) Weissleder, R.; Moore, A.; Mahmood, U.; Bhorade, R.; Benveniste, H.; Chiocca, E. A.; Basilion, J. P. In vivo magnetic resonance imaging of transgene expression. *Nat. Med.* **2000**, *6*, 351–354.

(9) Häfeli, U. O. Magnetic Nano- and Microparticles for Targeted Drug Delivery. In *Smart Nanoparticles in Nanomedicine: the MML Series*; Arshady, R.; Kono, K., Eds.; Kentus Books: London, UK, 2006; pp 77−126.

(10) Sako, M.; Hirota, S.; Ohtsuki, S. Clinical evaluation of ferromagnetic microembolization for the treatment of hepatocellular carcinoma. *Ann. Radiol.* **1985**, *29*, 200–204.

(11) Goodwin, S.; Peterson, C.; Hoh, C.; Bittner, C. Targeting and retention of magnetic targeted carriers (MTCs) enhancing intraarterial chemotherapy. *J. Magn. Magn. Mater.* **1999**, *194*, 132–139.

(12) Geschwind, J. F.; Kobeiter, H.; Peterson, C.; Leakakos, T. In *Magnetic Targeted Delivery of 90 Y to VX2 Rabbit Liver Tumors*; Society of Interventional Radiology: Salt Lake City, UT, 2003; p S70.

(13) Morimoto, Y.; Sugibayashi, K.; Okumura, M.; Kato, Y. Biomedical applications of magnetic fluids. I. Magnetic guidance of ferrocolloid-entrapped albumin microsphere for site specific drug delivery in vivo. *J. Pharmacobio-Dyn.* **1980**, *3*, 264–267.

(14) Ally, J.; Amirfazli, A.; Roa, W. Factors Affecting magnetic retention of particles in the upper airways: An in vitro and ex vivo study. *J. Aerosol Med.* **2006**, *19*, 491–509.

(15) Dames, P.; Gleich, B.; Flemmer, A.; Hajek, K.; Seidl, N.; Wiekhorst, F.; Eberbeck, D.; Bittmann, I.; Bergemann, C.; Weyh, T.; Trahms, L.; Rosenecker, J.; Rudolph, C. Targeted delivery of magnetic aerosol droplets to the lung. *Nat. Nanotechnol.* **2007**, *2*, 495–9.

(16) Pislaru, S. V.; Harbuzariu, A.; Gulati, R.; Witt, T.; Sandhu, N. P.; Simari, R. D.; Sandhu, G. S. Magnetically targeted endothelial cell localization in stented vessels. *J. Am. Coll. Cardiol.* **2006**, *48*, 1839–45.

(17) Pulfer, S. K.; Gallo, J. M. Enhanced brain tumor selectivity of cationic magnetic polysaccharide microspheres. *J. Drug Targeting* **1998**, *6*, 215–227.

(18) Reddy, G. R.; Bhojani, M. S.; McConville, P.; Moody, J.; Moffat, B. A.; Hall, D. E.; Kim, G.; Koo, Y. E.; Woolliscroft, M. J.; Sugai, J. V.; Johnson, T. D.; Philbert, M. A.; Kopelman, R.; Rehemtulla, A.; Ross, B. D. Vascular targeted nanoparticles for imaging and treatment of brain tumors. *Clin. Cancer Res.* **2006**, *12*, 6677–6686.

(19) Driscoll, C. F.; Morris, R. M.; Senyei, A. E.; Widder, K. J.; Heller, G. S. Magnetic targeting of microspheres in blood flow. *Microvasc. Res.* **1984**, *27*, 353–369.

(20) DeNardo, S. J.; DeNardo, G. L.; Miers, L. A.; Natarajan, A.; Foreman, A. R.; Gruettner, C.; Adamson, G. N.; Ivkov, R. Development of tumor targeting bioprobes (111In-chimeric L6 monoclonal antibody nanoparticles) for alternating magnetic field cancer therapy. *Clin. Cancer Res.* **2005**, *11*, 7087s–7092.

(21) Jurgons, R.; Seliger, C.; Hilpert, A.; Trahms, L.; Odenbach, S.; Alexiou, C. Drug loaded magnetic nanoparticles for cancer therapy. *J. Phys. Condens. Matter* **2006**, *18*, S2893–S2903.

(22) Lobel, D.; Hale, J. R.; Montgomery, D. B. A new magnetic technique for the treatment of giant retinal tears. *Am. J. Ophthalmol.* **1978**, *85*, 699–703.

(23) Holligan, D. L.; Gillies, G. T.; Dailey, J. P. Magnetic guidance of ferrofluidic nanoparticles in an in vitro model of intraocular retinal repair. *Nanotechnology* **2003**, *14*, 661–666.

(24) Asmatulu, R.; Zalich, M. A.; Claus, R. O.; Riffle, J. S. Synthesis, characterization and targeting of biodegradable magnetic nanocomposite particles by external magnetic fields. *J. Magn. Magn. Mater.* **2005**, *292*, 108–119.

(25) Mefford, O. T.; Woodward, R. C.; Goff, J. D.; Vadala, T. P.; St. Pierre, T. G.; Dailey, J. P.; Riffle, J. S. Field-induced motion of ferrofluids through immiscible viscous media: testbed for restorative treatment of retinal detachment. *J. Magn. Magn. Mater.* **2007**, *311*, 347Z–353.

(26) Plank, C.; Anton, M.; Rudolph, C.; Rosenecker, J.; Krotz, F. Enhancing and targeting nucleic acid delivery by magnetic force. *Expert Opin. Biol. Ther.* **2003**, *3*, 745–58.

(27) Mykhaylyk, O.; Antequera, Y. S.; Vlaskou, D.; Plank, C. Generation of magnetic nonviral gene transfer agents and magnetofection in vitro. *Nat. Protocols* **2007**, *2*, 2391–411.

(28) Morishita, N.; Nakagami, H.; Morishita, R.; Takeda, S.; Mishima, F.; Terazono, B.; Nishijima, S.; Kaneda, Y.; Tanaka, N. Magnetic nanoparticles with surface modification enhanced gene delivery of HVJ-E vector. *Biochem. Biophys. Res. Commun.* **2005**, *334*, 1121–1126.

(29) Gersting, S. W.; Schillinger, U.; Lausier, J.; Nicklaus, P.; Rudolph, C.; Plank, C.; Reinhardt, D.; Rosenecker, J. Gene delivery to respiratory epithelial cells by magnetofection. *J. Gene Med.* **2004**, *6*, 913–22.

(30) Mykhaylyk, O.; Zelphati, O.; Rosenecker, J.; Plank, C. siRNA delivery by magnetofection. *Curr. Opin. Mol. Ther.* **2008**, *10*, 493–505.

aggregation, and must also be biocompatible, nontoxic, and nonimmunogenic. Currently, the most often used biocompatible material for the preparation of magnetic particles is the iron oxide magnetite (Fe_3O_4), which is minimally toxic[31,32] and has been approved by the FDA as an MRI contrast agent.[2] A crucial aspect during the preparation of magnetite particles is to control their size distribution and prevent aggregation. This is possible with the help of coatings, which will, during the particle's application, also help to keep them finely dispersed and reduce nonspecific protein adsorption and clearance by macrophages. Coatings for magnetite particles include dextran,[33] silica,[34] oleate or oleic acid,[35,36] starch,[37] polyacrylamide,[38] poly(L-lactic acid),[39] and increasingly the nonantigenic polyethylene oxide (PEO).[40−42] The latter, which in the pharmaceutical world is called polyethylene glycol (PEG), has been used extensively in drug delivery as it improves hydrophilicity, minimizes aggregation, and is biocompatible.[43,44]

To allow magnetic drug delivery to the eye, we chose nanosized magnetite particles with a core size of 8−10 nm and protected them from aggregation with triblock copolymers made from PEO on both ends and central polyurethane units (Figure 1A).[45,46] The carboxylic acid functionality in the central urethane segment is essential to bind to the magnetite surface (Figure 1B), provide complete surface coverage, and maintain a well-dispersed particle suspension (Figure 1C). As the copolymer coating itself is not magnetic, we evaluated polymers of different chain length in order to find the one that allowed for good stability and would at the same time maximize the response to an applied magnetic field.

For *in vivo* magnetic drug delivery to the eye, a most important factor is the nontoxicity of the magnetic carrier particles. The aim of this study was to determine the biocompatibility of our magnetite nanoparticles coated with the PEO triblock copolymers in cells relevant for intraocular targeting. The first type of cells that our magnetic nanoparticles (MNPs) would encounter are the endothelial cells of the vascular system shortly after intravascular application and during magnetic targeting. As a surrogate for cells lining the blood vessels and capillaries, we grew human umbilical vein endothelial cells (HUVEC) and tested their viability upon addition of the MNPs in a colorimetric MTT (3-[4,5-dimethylthiazol-2yl]-2,5-diphenyltetrazolium bromide) assay. Once MNPs arrive in the capillary bed of the eye, they can be stopped magnetically and even brought to extravasate, based on experimental data from several groups.[11,47−49] Extravasation will get the MNPs into contact with other ocular cells such as retinal pigment epithelial cells. To explore the particles' toxicity in this environment, we chose human retinal pigment epithelial (HRPE) cells as a second

(31) Bacon, B. R.; Stark, D. D.; Park, C. H.; Saini, S.; Groman, E. V.; Hahn, P. F.; Compton, C. C.; Ferrucci, J. T. Ferrite particles: a new magnetic resonance imaging contrast agent. Lack of acute or chronic hepatotoxicity after intravenous administration. *J. Lab. Clin. Med.* **1987**, *110*, 164–171.

(32) Weissleder, R.; Stark, D. D.; Engelstad, B. L.; Bacon, B. R.; Compton, C. C.; White, D. L.; Jacobs, P.; Lewis, J. Superparamagnetic iron oxide: Pharmacokinetics and toxicity. *Am. J. Roentgenol.* **1989**, *152*, 167–173.

(33) Molday, R. S. Magnetic Iron-Dextran Microspheres. U.S. Patent 4452773, Jun 5, 1984.

(34) Liu, Q.; Xu, Z.; Finch, J. A. In *Silica Coatings on Nanosize Superparamagnetic Particles*, Canadian Chemical Engineering Conference, Edmonton, Canada, 1997; The Chemical Institute of Canada: Ottawa, Canada; p 744.

(35) Hyeon, T. Chemical synthesis of magnetic nanoparticles. *Chem. Commun.* **2003**, *8*, 927–934.

(36) Morales, M. A.; Jain, T. K.; Labhasetwar, V.; Leslie-Pelecky, D. L. Magnetic studies of iron oxide nanoparticles coated with oleic acid and Pluronic block copolymer. *J. Appl. Phys.* **2005**, *97*, 10Q905.

(37) Park, S. I.; Lim, J. H.; Kim, J. H.; Yun, H. I.; Roh, J. S.; Kim, C. G.; Kim, C. O. Effects of surfactant on properties of magnetic fluids for biomedical application. *Phys. Status Solidi B* **2004**, *241*, 1662–1664.

(38) Sun, H.; Zhang, L.; Zhang, X.; Zhang, C.; Wei, Z.; Yao, S. 188Re-labeled MPEG-modified superparamagnetic nanogels: preparation and targeting application in rabbits. *Biomed. Microdevices* **2008**, *10*, 281–287.

(39) Zhao, H.; Saatchi, K.; Häfeli, U. O. Preparation of biodegradable magnetic microspheres with poly(lactic acid) coated magnetite. *J. Magn. Magn. Mater.* **2009**, *321*, 1356–1363.

(40) Barrera, C.; Herrera, A. P.; Rinaldi, C. Colloidal dispersions of monodisperse magnetite nanoparticles modified with poly(ethylene glycol). *J. Colloid Interface Sci.* **2009**, *329*, 107–113.

(41) Liu, X. Q.; Kaminski, M. D.; Riffle, J. S.; Chen, H.; Torno, M.; Finck, M. R.; Taylor, L. T.; Rosengart, A. J. Preparation and characterization of biodegradable magnetic carriers by single emulsion solvent evaporation. *J. Magn. Magn. Mater.* **2007**, *311*, 84–87.

(42) Hu, F.; Li, Z.; Tu, C.; Gao, M. Preparation of magnetite nanocrystals with surface reactive moieties by one-pot reaction. *J. Colloid Interface Sci.* **2007**, *311*, 469–474.

(43) Greenwald, R. B. PEG drugs: an overview. *J. Controlled Release* **2001**, *74*, 159–171.

(44) Gref, R. Surface-Engineered Nanoparticles as Drug Carriers. In *Synthesis, Functionalization and Surface Treatment of Nanoparticles*; Baraton, M. I., Ed.; American Scientific Publishers: Stevenson Ranch, CA, 2003.

(45) Harris, L. A.; Goff, J. D.; Carmichael, A. Y.; Riffle, J. S.; Harburn, J. J.; St. Pierre, T. G.; Saunders, M. Magnetite nanoparticle dispersions stabilized with triblock copolymers. *Chem. Mater.* **2003**, *15*, 1367–1377.

(46) Zhang, Q.; Thompson, M. S.; Carmichael-Baranauskas, A. Y.; Caba, B. L.; Zalich, M. A.; Lin, Y. N.; Mefford, O. T.; Davis, R. M.; Riffle, J. S. Aqueous dispersions of magnetite nanoparticles complexed with copolyether dispersants: experiments and theory. *Langmuir* **2007**, *23*, 6927–6936.

(47) Meyers, P. H.; Cronic, F.; Nice, C. M. Experimental approach in the use and magnetic control of metallic iron particles in the lymphatic and vascular system of dogs as a contrast and isotopic agent. *Am. J. Roentgenol. Radium Ther. Nucl. Med.* **1963**, *90*, 1068–1077.

(48) Clement, O.; Rety, F.; Cuenod, C. A.; Siauve, N.; Carnot, F.; Bordat, C.; Siche, M.; Frija, G. MR lymphography: evidence of extravasation of superparamagnetic nanoparticles into the lymph. *Acad. Radiol.* **1998**, *5 Suppl 1*, S170–172.

(49) Weissleder, R.; Bogdanov, A.; Tung, C. H.; Weinmann, H.-J. Size optimization of synthetic graft copolymers for in vivo angiogenesis imaging. *Bioconjugate Chem.* **2001**, *12*, 213–219.

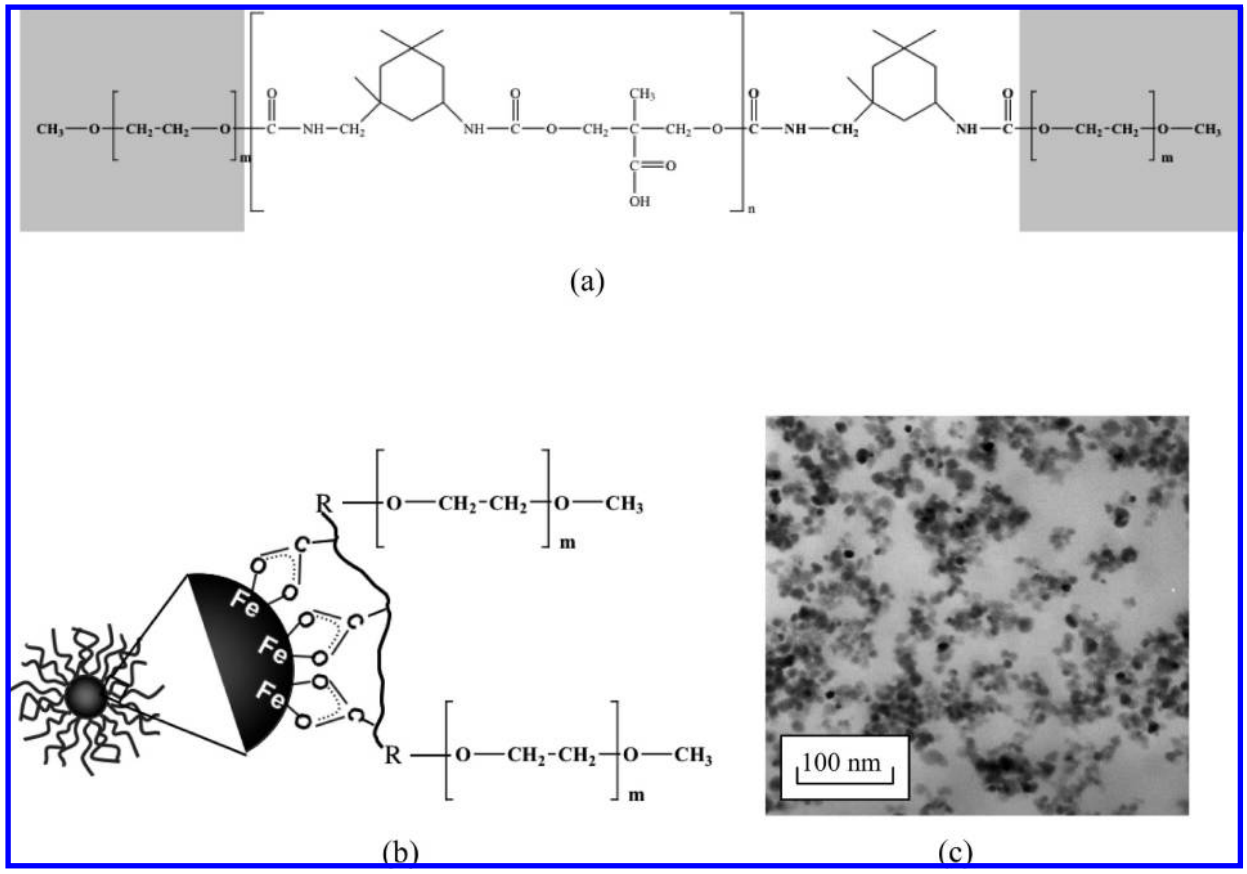

Figure 1. (a) Poly(ethylene oxide) triblock copolymer containing carboxylic acid functionality in the central urethane segment ($n = 3$, 5, or 10). m was varied to investigate the effects of tailblock length on toxicity. (b) Schematic depicting the binding of the carboxylic acid moieties onto the iron oxide nanoparticle surface. Steric stabilization of the particles in the cell culture medium was achieved through extension of the hydrophilic poly(ethylene oxide) tail blocks from the magnetite surface into the medium. (c) Transmission electron micrograph of magnetite nanoparticles coated with the 5K-3-5K copolymer.

cell type. Furthermore, the treatment of intraocular tumors is another potential drug delivery target, and we thus evaluated cancer cells as additional test cells. Although metastases from prostate cancer are rare in the eye,[50,51] we chose the PC3 and C4-2 prostate cancer cells because they are sensitive toward toxic effects in the MTT assay and are thus good indicator cells for potential toxic effects. In addition to cell viability measurements, we evaluated the MNP interaction with the different cell types over time using confocal microscopy.

Materials and Methods

Magnetic Nanoparticle Preparation and Analysis. Magnetic nanoparticles (MNPs) of around 10 nm in diameter were prepared using Massart's method of mixing Fe(II) and Fe(III) in aqueous ammonia.[52] The particles' surface was immediately coated with a hydrophilic triblock copolymer, which consisted of two PEO end blocks and contained defined concentrations of carboxylic acid functional groups (PEO-COOH-PEO) in the central segments (Figure 1).[45] The nomenclature that has been adopted to describe these copolymers is the number average molecular weight of PEO (M_n) in kDa, followed by the average number of carboxylic acid groups in the central segment, and then by the M_n of the second PEO molecule; e.g., 2K-3-2K. The detailed synthesis of the copolymers and the MNPs, and the subsequent method for their coating with the block copolymers have previously been reported.[45] In short, MNPs were prepared via bulk coprecipitation of aqueous solutions of $FeCl_3 \cdot 6H_2O$ (0.389 M, 2.0 g) and $FeCl_2 \cdot 4H_2O$ (0.195 M, 0.736 g) in a three-neck, 250-mL, round-bottom flask equipped with a mechanical stirrer and pH electrode connected to a pH meter under an inert nitrogen environment. Immediately after the addition of the aqueous iron salts, NH_4OH (50% v/v aqueous) was quickly syringed into the

(50) Holland, D.; Maune, S.; Kovacs, G.; Behrendt, S. Metastatic tumors of the orbit: a retrospective study. *Orbit* **2003**, *22*, 15–24.
(51) Barbon, J. J.; Gonzalez-Tuero, J.; Gay, L. L.; Perez-Garcia, F. J.; Sampedro, A. Regression of a choroidal metastasis from prostate adenocarcinoma after hormonal therapy. *Arch. Soc. Esp. Oftalmol.* **2007**, *82*, 715–717.
(52) Massart, R. Magnetic Fluids and Process for Obtaining Them. U.S. Patent 4,329,241, May 11, 1980.

flask and stirred until a pH of 9.5 was reached (10 mL). The dispersion quickly turned bluish-green and then black, indicating the formation of magnetite. Nucleation and growth of magnetite particles was allowed to occur for 30 min with stirring under a N_2 atmosphere. After this, the N_2 flow was removed, and a solution of 2 g of PEO-COOH-PEO polymer dissolved in 25 mL of CH_2Cl_2 was syringed into the flask and allowed to interact with the magnetite for 30 min with stirring (pH 8.5−9). The CH_2Cl_2 was removed with a strong N_2 flow over 2 h, and the polymer−magnetite nanoparticle aqueous suspension was neutralized with 25% v/v aqueous HCl to pH 6.5−7. The resultant stable colloidal dispersion was transferred to a dialysis membrane (Spectra pore 7, MWCO 1000) and dialyzed against water for 3 days, refreshing the dialysis water twice per day. Any particle aggregates in the salt-free magnetite ferrofluids were removed by centrifuging for 30 min intervals where the sediment was discarded and the process repeated until little to no precipitation was observed in the bottom of the centrifuge tube.

The magnetic properties of the polymer-coated magnetite nanoparticles were measured in their solid state at room temperature using a Standard 7300 Series Lake Shore Cryotronics vibrating sample magnetometer (VSM; Westerville, OH, U.S.A.). The magnetic moment of each dried sample was measured over a range of applied fields from −8000 to +8000 Oe with a sensitivity of 0.1 emu. Particle mass specific magnetizations were taken from the responses at +8000 Oe. The polymer coated magnetite nanoparticles were imaged with a Philips 420T transmission electron microscope (TEM) operating at 100 kV. Dilute aqueous dispersions of the nanoparticles were deposited on a carbon paper coated copper TEM grid and then air-dried for imaging. The particle sizes were obtained by measuring and averaging the largest dimension of 100−200 individual particles within at least two regions of the micrograph. Sizes taken within different regions were similar. It was not possible to distinguish the polymer coatings from the magnetite in these images.

Cell Culture. Human umbilical vein endothelial cells (HUVEC; Cambrex Corporation, East Rutherford, NJ, U.S.A.) were grown in a commercially supplied growth factor rich media (EGM-2 Bulletkit; CC-3162; Cambrex Corporation). Human retinal pigment epithelial (HRPE) cells were received from Case Western Reserve University hospital and grown in media prepared by adding 22.5 mL of 15% fetal bovine serum, 15 μL of 5 μg/mL gentamicin, and 1.5 mL of 2.5 μg/mL amphotericin B to 126 mL of Dulbecco's modification of Eagle's medium with low glucose content (1 g/L) (DMEM-L; Mediatech, Herndon, VA). The metastatic human prostate adenocarcinoma cells C4-2 were grown in RPMI-1640 complete (Mediatech) with 10% fetal bovine serum added. A second type of prostate cancer cells, the androgen independent and androgen receptor negative PC3 (American type Culture Collection, Manassas, VA, U.S.A.), was grown in media with F-12 nutrient mixture (Invitrogen 21700-075), 1% penicillin/streptomycin (1000 units/10,000 μg/mL) (Invitrogen 151400-122), and 10% fetal bovine serum (Invitrogen 10437-028). All cells were grown at 37 °C and 5% CO_2, with media changes done every 2−3 days.

MTT Assay. The *in vitro* cytotoxicity of magnetic nanoparticles was tested using a modified cell viability assay.[53] The MTT assay is a colorimetric assay for which 5000 cells were plated, in 100 μL of media, into each well of a 96-well plate and incubated for 24 h. Fifty microliters of magnetite and/or polymer suspended at concentrations up to 5 mg/mL in media were added and incubated for 48 h. The supernatant was carefully removed, and 100 μL of media and 20 μL of a 5 mg/mL MTT solution added and incubated for 3 more hours. Viable cells take up the MTT into their mitochondria and metabolize it into blue formazan crystals. As a control, 150 μL of PBS at pH 7.4 was added to cells in 8 of the wells. The supernatant in each well was aspirated and 150 μL of dimethyl sulfoxide (DMSO) added to solubilize the cells and MTT crystals. After 1 h of shaking on an Eppendorf Thermomixer at 37 °C and 400 rpm to dissolve all crystals, the blue color was read in a multiwell scanning spectrophotometer at 540 nm. The cell viability was calculated by comparing the sample absorption to the one of the control cells, which was by definition 100%.

Higher concentrations of magnetic nanoparticles are dark brown and interfere with the spectrophotometry readings when taken up by the cells. The net readings were therefore corrected with a net particle reading, which was obtained by employing a column of 8 wells that contained the same amount of cells and particles and had undergone the same washing steps, but had not received the MTT solution. Magnetic nanoparticles were considered toxic if the difference between cell growth inhibition of control and exposed cells was statistically significant at the 5% level, as determined by a *t*-test.

Cell Staining and Confocal Microscopy. Cell suspensions were prepared at a concentration of 1×10^5 per mL of media and 1.5 mL added to 6 well plates each containing an autoclaved 22 mm × 22 mm glass slide insert coated with lysine. On the next day, 1.5 mL of the sterile filtered magnetic nanoparticle suspensions or the gas-sterilized polymer controls at a concentration of 2.5 mg/mL cell media were added to each of the wells with firmly attached cells. At different time points (1 h, 3, 8, and 24 h, 2 and 3 days), the media was removed from the wells and the cells carefully washed with phosphate buffered saline (PBS). In a first step, 1.5 mL of media containing LysoTracker Green DND-26 (2 μL of a 1 mM DMSO solution dissolved in 40 mL of media; Molecular Probes, Eugene, Oregon, U.S.A.) was added to the wells and left for 30 min. Three hundred microliters of media containing FAST DiI (6 μL of a 40% ethanolic FAST DiI solution per mL of media; Molecular Probes) was added, gently shaken for 30 s, and incubated for another 5 min. The supernatant was then removed, the cells washed twice with PBS, and the glass slides immersed

(53) Pieters, R.; Huismans, D. R.; Leyva, A.; Veerman, A. J. P. Comparison of the rapid automated MTT-assay with a dye exclusion assay for chemosensitivity testing in childhood leukaemia. *Br. J. Cancer* **1989**, *59*, 217–220.

Table 1. Physico-Chemical Properties of the Magnetic Nanoparticles Coated with Triblock Copolymer

name	triblock copolymer composition (PEO M_n − number of COOH groups − PEO M_n)	magnetite concentration (wt%)	saturation magnetization (emu/g at 8000 Oe)	particle size (nm ± S.D.)
MNP 0.75K-3-0.75K	770−2.6−770	45.4	34	8.8±2.7
MNP 2K-3-2K	1930−3.1−1930	37.4	20	*
MNP 5K-3-5K	4845−2.5−4845	30.2	20	*
MNP 15K-3-15K	16470−3−16470	6.9	5	*

*It was not possible to measure the overall particle size by TEM. The magnetite core size, however, was identical to that of the MNP 0.75K-3-0.75K.

in 10% buffered formaldehyde for 15 min. A drop of Vectashield mounting medium with DAPI (Vector Laboratories, Burlington, Ontario, Canada) was added to a microscope slide and the coverslip placed on it, cell side down. Edges were sealed with nail polish (Wet and Wild, Markwins Beauty Products Inc., California, U.S.A.). Confocal microscopy was performed on a Leica TCS-SP2 AOBS Laser Scanning Confocal Microscope (Heidelberg, Germany) using a 60× oil immersion lens with argon laser at 488 nm to detect the nuclei and a green HeNe laser at 543 nm to detect the lysosomes and mitochondria. In addition, light reflected off high-density magnetite from the nanoparticles was detected by physically putting a detector under the laser line on the built-in spectrophotometer and turning on the reflection mode on the acousto-optical tunable filter (AOTF) button. This mode allows the detection of objects (MNPs) smaller than 200 nm, although resolving them is not possible.

Results

The preparation of MNPs, using Massart's method immediately followed by coating with the different triblock copolymers, resulted in easily dispersed, nonagglomerated MNPs. The MNPs coated with 5K-3-5K are shown in Figure 1C. The excellent dispersibility of all MNPs suggests that, as expected, the triblock copolymer bound to the magnetite surface through its central carboxylic groups and that the PEO-tail pointed outward from the particle surface, as shown schematically in Figure 1B. The physical properties of the investigated MNPs are given in Table 1. The size of the magnetite cores as measured by TEM was similar in all preparations. The coating thickness, however, went up with longer PEO tail blocks, as shown indirectly by the steady decrease in the magnetic susceptibility of the MNPs (Table 1).

We tested the effects of three different MNPs on HUVECs and on PC3 cancer cells (Figures 2B and 3B). For both cell types, the order of increasing toxicity was the same: MNPs 15K-3-15K (20%) were less toxic than MNPs 5K-3-5K (30%), which were less toxic than MNPs 2K-3-2K (30% and 50%). In other words, MNPs coated with longer PEO tail blocks were less cell toxic than MNPs coated with shorter chain PEOs. The order of increasing toxicity for the pure polymers in the same two cell lines was identical: Polymer 5K-3-5K was less toxic than polymer 2K-3-2K, which was less toxic than polymer 0.75K-3-0.75K (Figures 2A and 3A). Quantitatively, the pure polymers were several fold more toxic than the magnetite nanoparticles (Table 2).

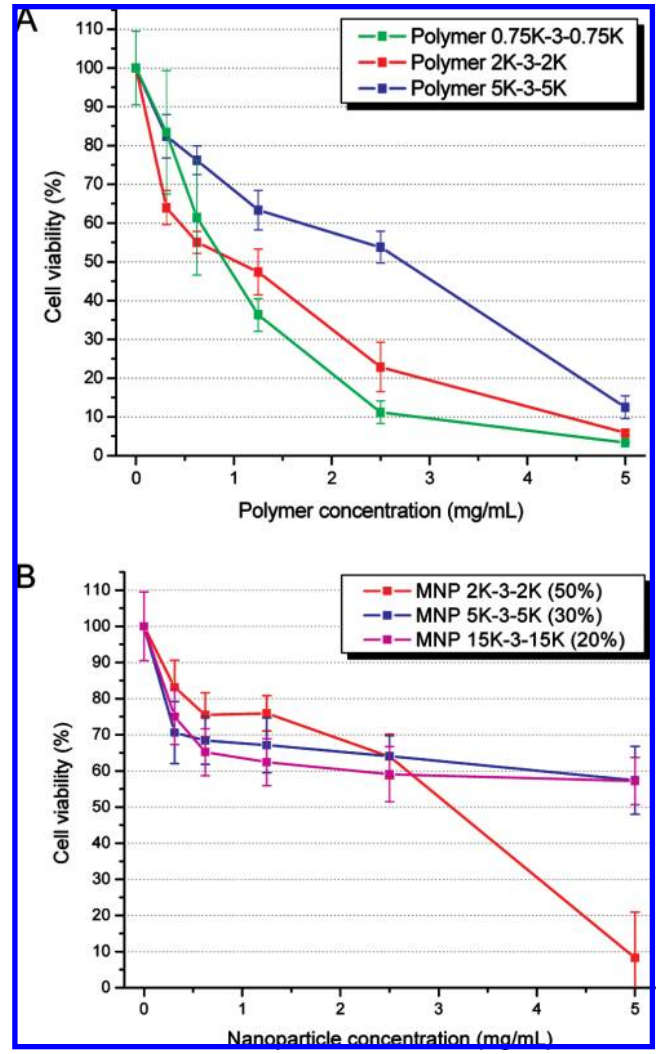

Figure 2. Cell viability of HUVEC cells measured after adding increasing concentrations of (A) pure triblock copolymers or (B) magnetite nanoparticles coated with the triblock copolymers.

All pure triblock copolymers and the coated magnetite nanoparticles displayed concentration dependent toxic effects (Figures 2 and 3). The concentration of the magnetite core, however, was not found to be important in terms of toxicity. Specifically, MNP 2K-3-2K (30%) and MNP 2K-3-2K (50%) exhibited no significantly different cell viabilities upon incubation with PC3 cancer cells (Figure 3B).

In an additional experiment, the same MNPs at the highest concentration of 5 mg/mL were incubated with two additional

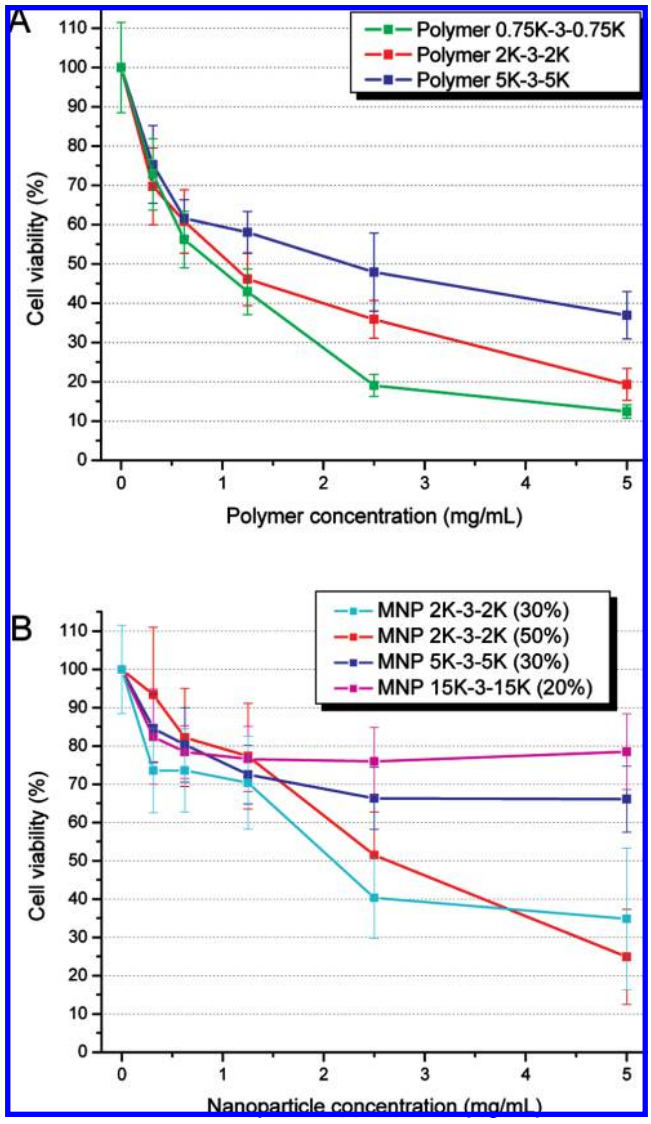

Figure 3. Cell viability of PC3 prostate cancer cells measured after adding increasing concentrations of (A) pure triblock copolymers or (B) magnetite nanoparticles coated with the triblock copolymers.

Table 2. Inhibitory Dose ID_{50} Concentrations (mg/mL) for MNPs and Pure Polymers in Different Types of Cells[a]

	PC3	HUVEC	HRPE	C4-2
Polymer 0.75K-3-0.75K	0.94	0.90	*	0.98
Polymer 2K-3-2K	1.10	1.07	*	>5
Polymer 5K-3-5K	2.28	2.75	*	≫5
MNP 0.75K-3-0.75K (30%)	*	*	>5	2.91
MNP 2K-3-2K (30%)	2.10	*	>5	3.52
MNP 2K-3-2K (50%)	2.63	3.12	*	*
MNP 5K-3-5K (30%)	>5	>5	≫5	≫5
MNP 15K-3-15K (20%)	≫5	>5	≫5	≫5

[a] (*) not determined.

cell types, prostate cancer C4-2 cells and human retinal pigment epithelial (HRPE) cells. The cell viabilities as measured by the MTT assay were similar to those found with the PC3 cells and the HUVECs. Coating the MNPs with 5K-3-5K and 15K-3-15K PEO-chain-containing block co-

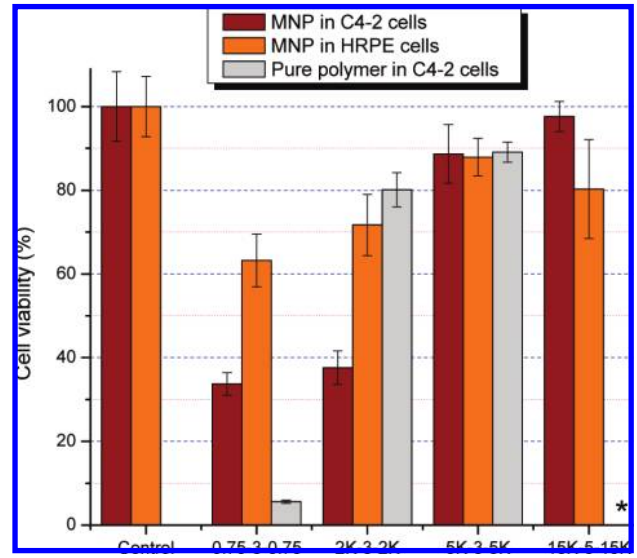

Figure 4. Dependence of magnetic nanoparticle toxicity on PEO tail length. The MNP and polymer concentration was 5 mg/mL for all measurements. *, not determined.

polymers only slightly lowered the cell viabilities, while both the 2K-3-2K and 0.75K-3-0.75K coatings significantly reduced viability (Figure 4).

Microscopic observations of the cells after the addition of the different polymers or the polymer-coated MNPs confirmed the MTT data. The most toxic MNPs were the ones coated with the short chain PEO 0.75K-3-0.75K. Within hours, many cells started to show the typical signs of apoptosis[54] including blebbing of the nucleus and condensing of the chromatin (Figure 5). After 72 h, the density of the surviving cells was starkly reduced. The signs of apoptosis were seen in all tested cell types. The MNP 2K-3-2K also showed a few apoptotic events but at much reduced frequencies. The confocal microscopy picture of these MNPs in C4-2 cells after 8 h looked rather normal (Figure 6).

The addition of each of the coated MNPs to the cells resulted in a rapid adherence of nanoparticles to the cells' surfaces followed by the uptake of single particles and internalization into the cytoplasm of the cells (Figure 6). MNPs with longer-chain PEOs were not found to be toxic to the cells: After 24 h, many of the MNPs 5K-3-5K were found inside the cells of C4-2 prostate cancer cells (Figure 7). The even longer-chain MNPs 15K-3-15K were most rapidly taken up by the HRPE cells. After 72 h, the end point of the incubation experiment, all nanoparticles were found inside the cells, with no growth inhibition visible at all (Figure 8). The PEO coating seemed to considerably enhance MNP uptake, as uncoated control MNPs agglomerated rapidly under cell culture conditions and were internalized only minimally (Figure 9).

Discussion

Magnetite and maghemite are naturally occurring biocompatible and nontoxic inorganic iron oxides. For

(54) Wyllie, A. H.; Kerr, J. F. R.; Currie, A. R. Cell death: The significance of apoptosis. *Int. Rev. Cytol.* **1980**, *68*, 251–306.

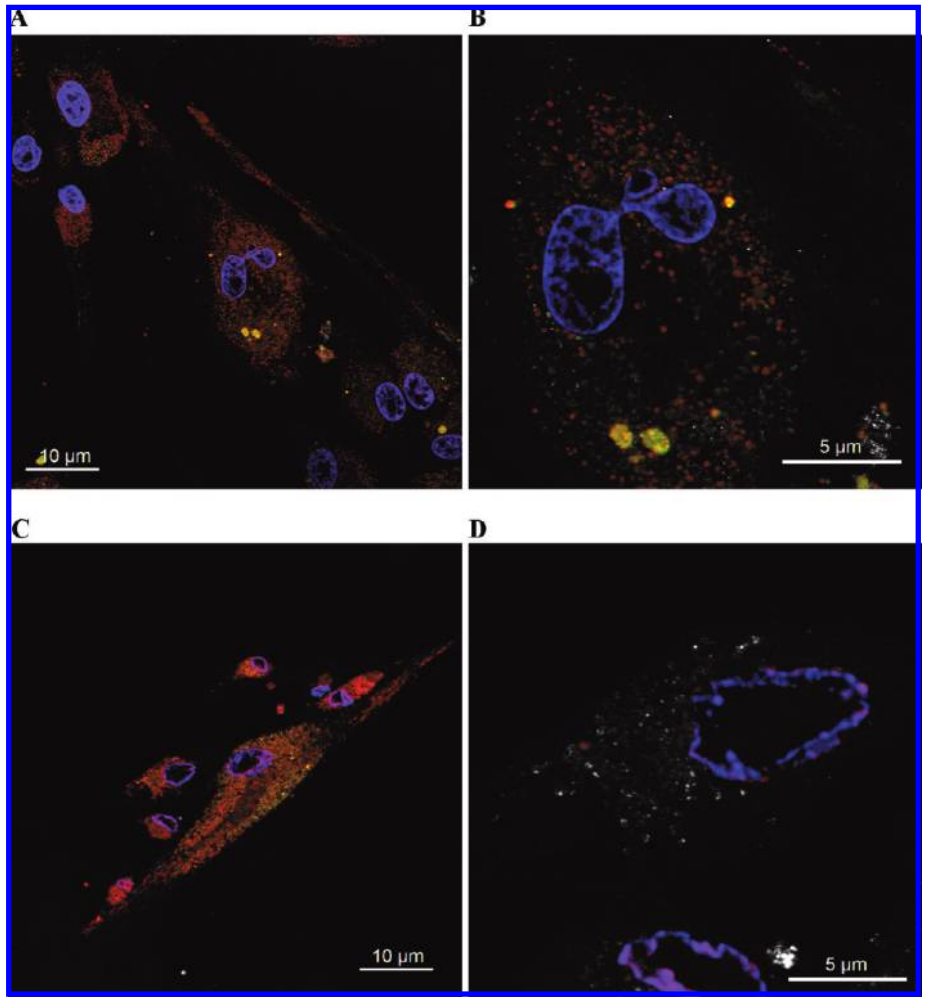

Figure 5. MNPs 0.75K-3-0.75K with short PEO tails are cytotoxic to HRPE cells. Signs for toxicity and ongoing apoptosis are (A, B) blebbing nuclei after 24 h of incubation and (C, D) condensed chromatin photographed after 48 h of incubation.

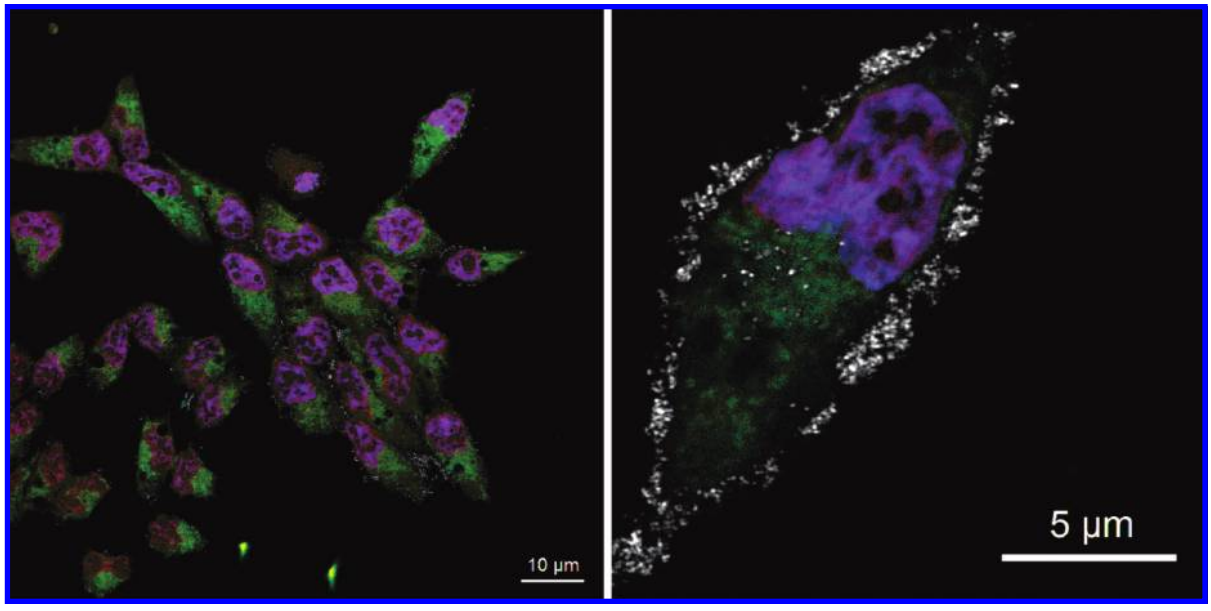

Figure 6. Uptake of MNP 2K-3-2K (30%) (5 mg/mL) by C4-2 prostate cancer cells after 8 h of incubation.

millions of years they have been grown inside magnetotactic bacteria[55] and have more recently been proven unequivocally to occur in pigeons, honey bees, and humans.[56,57] Given that these iron oxides occur naturally

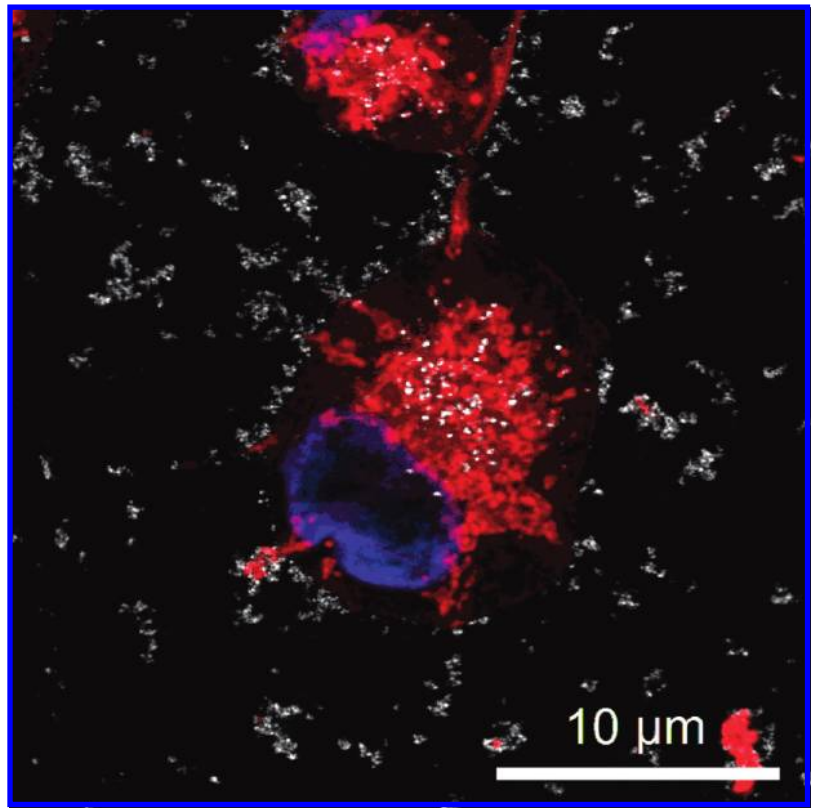

Figure 7. Uptake of MNP 5K-3-5K (30%) (5 mg/mL) by C4-2 prostate cancer cells after 24 h of incubation was rapid and showed no signs of toxicity. The entire set of 1 μm slices of confocal microscopy pictures can be seen as a movie in Supporting Information.

in the form of nanosized crystals, using magnetite and maghemite nanoparticles for magnetic drug targeting and as contrast agents, for example, would thus seem to be straightforward and biologically harmless. There is, however, one problem with their direct use. Magnetite and maghemite nanoparticles easily agglomerate and thus cannot be directly used. To obtain defined submicrometer size suspensions and to use them *in vitro* and *in vivo*, the magnetic particles have to be coated with materials that keep the particles apart. Such coating materials include carbohydrates, polymers, silica, metals, and peptides/proteins.

In our work, we prepared dispersions of superparamagnetic nanoparticles coated with a PEO-polyurethane-PEO triblock copolymer for future use in ocular drug targeting. The MNP suspensions thus prepared were of narrow size distribution, truly superparamagnetic, and showed no evidence of aggregation (Figure 1). Since the polymer coatings had not previously been tested for cytotoxic effects, they were evaluated in an MTT cell viability assay with relevant cell types.

MNPs coated with longer-chain triblock copolymers (5 and 15 kDa) were found to be nontoxic to endothelial (HUVEC), epithelial (HRPE), and tumor (PC3 and C4-2) cells. The inhibitory dose that resulted in 50% cell viability, the ID_{50}, was calculated from the curves in Figures 2−4 and was found to be above, and often far above, 5 mg of MNPs per milliliter of cell media (Table 2). The maximal MNP concentration of 5 mg/mL was chosen to be at least 10× higher than any MNP concentration foreseen to be used for ocular magnetic targeting. Most authors who have reported on the toxicity of MNPs employed much smaller test amounts, (e.g., up to 10 mg/kg for *in vivo* MR imaging studies,[58−60] up to 25 μg/mL for magnetic transfection studies,[61−63] and up to 1 mg/mL for different *in vitro* cell studies[60,64]). Using the high MNP

(55) Schüler, D.; Frankel, R. B. Bacterial magnetosomes: microbiology, biomineralization and biotechnological applications. *Appl. Microbiol. Biotechnol.* **1999**, *52*, 464–473.

(56) Kirschvink, J. L.; Kobayashi-Kirschvink, A.; Diaz-Ricci, J. C.; Kirschvink, S. J. Magnetite in human tissues: A mechanism for the biological effects of weak ELF magnetic fields. *Bioelectromagnetics* **1992**, *Suppl. 1*, 101–113.

(57) Collingwood, J. F.; Chong, R. K.; Kasama, T.; Cervera-Gontard, L.; Dunin-Borkowski, R. E.; Perry, G.; Posfai, M.; Siedlak, S. L.; Simpson, E. T.; Smith, M. A.; Dobson, J. Three-dimensional tomographic imaging and characterization of iron compounds within Alzheimer's plaque core material. *J. Alzheimers Dis.* **2008**, *14*, 235–245.

(58) Muldoon, L. L.; Sandor, M.; Pinkston, K. E.; Neuwelt, E. A. Imaging, distribution, and toxicity of superparamagnetic iron oxide magnetic resonance nanoparticles in the rat brain and intracerebral tumor. *Neurosurgery* **2005**, *57*, 785–96.

(59) Chouly, C.; Pouliquen, D.; Lucet, I.; Jeune, J. J.; Jallet, P. Development of superparamagnetic nanoparticles for MRI: effect of particle size, charge and surface nature on biodistribution. *J. Microencapsul.* **1996**, *13*, 245–255.

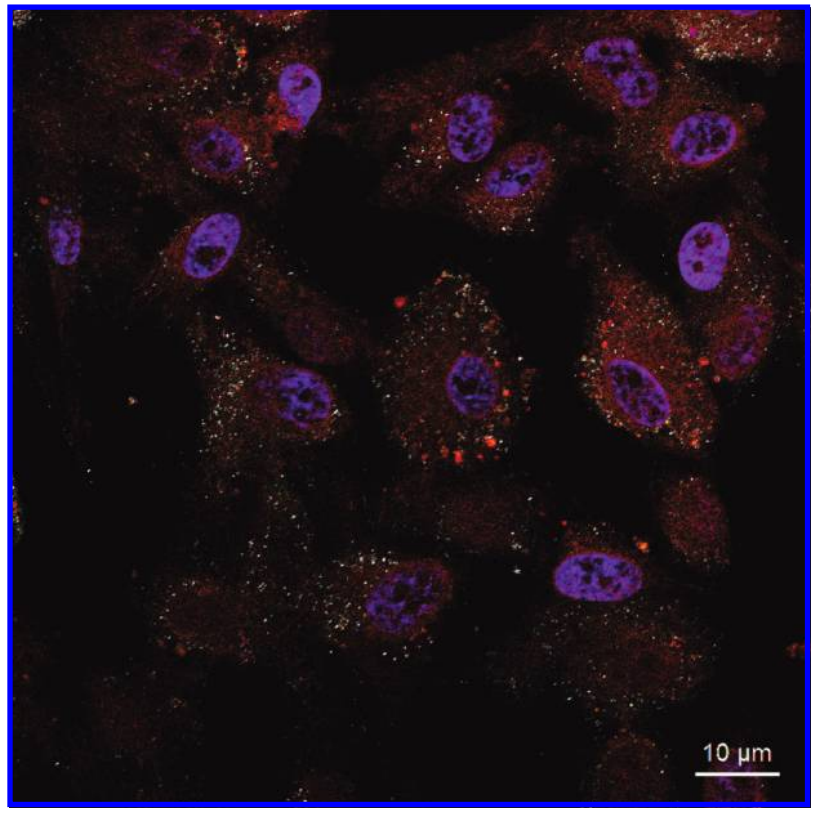

Figure 8. Although HRPE cells took up large amounts of the MNPs, they were not sensitive toward the higher molecular weight polymer coatings. This picture shows healthy HRPE cells 72 h after adding the highest concentration (5 mg/mL) of MNPs 15K-3-15K (30%).

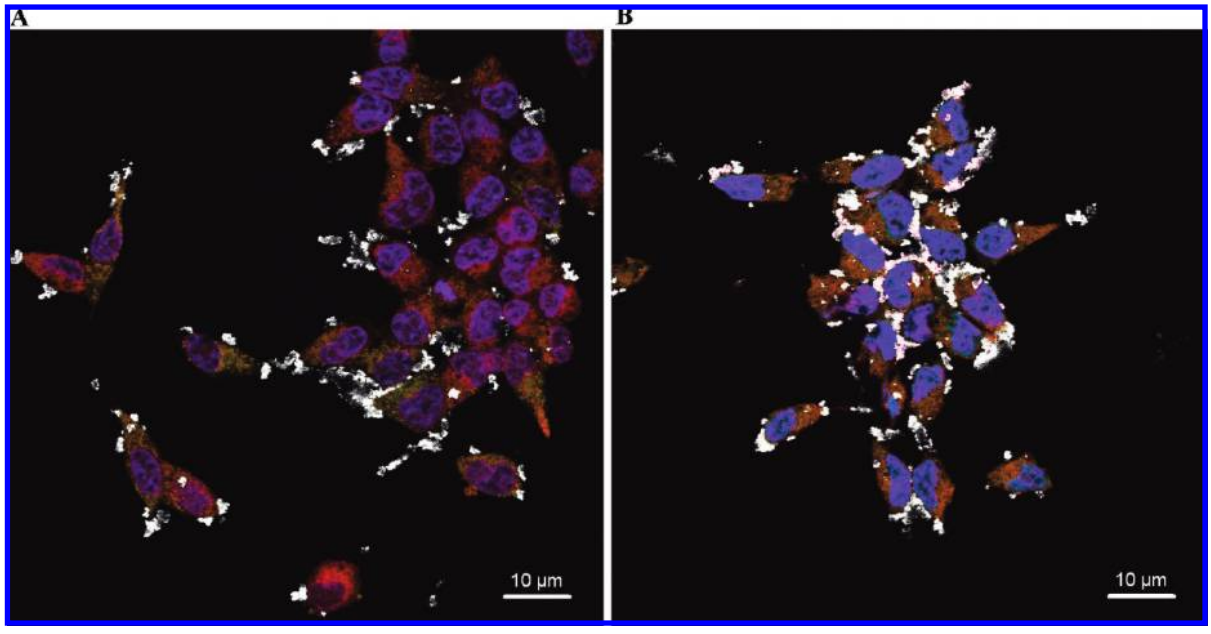

Figure 9. Uncoated MNPs (5 mg/mL) agglomerated rapidly and showed only minor uptake into C4-2 prostate cancer cells. The pictures were taken (A) 3 h and (B) 24 h after the addition of the nanoparticles.

concentration of 5 mg/mL for the tests gives us confidence that we are not overlooking any toxic effects.

Unlike MNPs coated with long-chain copolymers, the toxicity tests of the MNPs coated with the 2K-3-2K and even more so the 0.75K-3-0.75K copolymer, clearly showed dose-dependent toxic effects (Figures 2−4). This was strikingly obvious in the confocal microscopy studies where many of the cells (all types) developed apoptotic figures and showed chromatin condensation (Figure 5). The toxic effects did not correlate with MNP uptake, as all cell types pinocytosed or

phagocytosed the MNPs with different coatings at similar rates, showing increasing numbers of MNPs inside their cytoplasm at later time points (see, for example, Figures 7 and 8). Such facile cellular uptake of MNPs has been reported by other authors working with MNPs for use in hyperthermia,[65] cancer diagnosis and biodistribution studies,[66] and cancer therapy.[67] The uptake could be further enhanced and made more specific, for example, to efficiently detect gene expression, with MNPs containing additional shuttle groups, such as the tat domain,[8,68] RGD-peptides, bombesin analogues, and many others.[69,70]

It has been reported that MNPs are normally ingested via endocytosis into phagosomes, which then eventually fuse with lysosomes for degradation.[71] To investigate this route, we attempted to show where the MNPs were located inside the cell after uptake by staining the lysosomes with LysoTracker (see the red vesicles, for example in Figure 7). The MNPs, however, could not be located directly inside these vesicles. Further experiments will be necessary to pinpoint the uptake mechanism.

The most cytotoxic compounds in our tests were the pure polymers (Figures 2A and 3A, and Table 2). As with the coated MNPs, the smallest molecular weight triblock copolymer 0.75K-3-0.75K was the most toxic, followed in decreasing cytotoxicity by the 2K-3-2K and the 5K-3-5K. Binding the copolymers to the surface of MNPs very likely reduced the toxic effects not only due to the diminishing overall amount of the copolymer but also due to the different configuration the copolymer is in when bound to the MNP surface. The pure copolymer might have surface activity and even form micelle-like structures, something that would not be the case when the polyurethane backbone is tightly bound to the MNPs. Since no critical micelle concentration data is available, this is currently a hypothesis and will have to be confirmed in future experiments.

Our finding that short-chain copolymers are cytotoxic and much more so than long-chain copolymers of the same type is not unique. Zange et al. saw similar toxic effects with PLGA-PEO-PLGA copolymers.[72] They reported highly toxic effects in L929 fibroblast cells when they used a copolymer with a 1 kDa PEO unit, whereas essentially no toxicity (MTT viability of 80−100%) was seen in 4 kDa and 10 kDa PEO unit copolymers. Furthermore, Park et al. reported that oleic acid is nontoxic up to 8% of the blood volume, while the shorter-chain decanoic and nonanoic acids are already toxic at 0.5%.[37] All these fatty acids are used as coatings of MNPs.

Our finding that shorter polymer tails are more toxic than longer ones does not easily translate to the *in vivo* world as the mechanism of toxicity is not currently known. One might expect that even the longer polymer coatings could convert from less toxic to more toxic molecules if they become degraded in the target tissue by enzymatic or hydrolytic action. For the currently tested copolymers, however, we expect such degradation processes to be minimal since the ether groups of PEO are rather stable, and the ester and amide bonds on the surface of the magnetite nanoparticles are protected from enzymatic attack.

The content of magnetite within the MNPs does not seem to have a significant impact on cell viability. In Figure 3B, the curves for MNP 2K-3-2K (30%) and for MNP 2K-3-2K (50%) are not statistically different. Both MNPs possess identical PEO end blocks but differ in their iron oxide content. This suggests that the main factor for toxicity is the polymer coating and not the magnetite core. Successful magnetic targeting requires a large magnetic moment, and the finding that an increased amount of the magnetic component does not increase toxicity is thus desirable.

(60) Kim, J. S.; Yoon, T. J.; Yu, K. N.; Kim, B. G.; Park, S. J.; Kim, H. W.; Lee, K. H.; Park, S. B.; Lee, J. K.; Cho, M. H. Toxicity and tissue distribution of magnetic nanoparticles in mice. *Toxicol. Sci.* **2006**, *89*, 338–347.

(61) Arbab, A. S.; Liu, W.; Frank, J. A. Cellular magnetic resonance imaging: current status and future prospects. *Expert Rev. Med. Devices* **2006**, *3*, 427–439.

(62) Arbab, A. S.; Wilson, L. B.; Ashari, P.; Jordan, E. K.; Lewis, B. K.; Frank, J. A. A model of lysosomal metabolism of dextran coated superparamagnetic iron oxide (SPIO) nanoparticles: implications for cellular magnetic resonance imaging. *NMR Biomed.* **2005**, *18*, 383–389.

(63) Choi, H.; Choi, S. R.; Zhou, R.; Kung, H. F.; Chen, I. W. Iron oxide nanoparticles as magnetic resonance contrast agent for tumor imaging via folate receptor-targeted delivery. *Acad. Radiol.* **2004**, *11*, 996–1004.

(64) Gref, R.; Couvreur, P.; Barratt, G.; Mysiakine, E. Surface-engineered nanoparticles for multiple ligand coupling. *Biomater.* **2003**, *24*, 4529–4537.

(65) Jordan, A.; Scholz, R.; Schnoy, N.; Wust, P.; Maier-Hauff, K.; Felix, R. Differential endocytosis of magnetic fluid particles into human primary glioblastoma, neuronal and fibroblast cells in vitro. *Eur. J. Cell Biol.* **1997**, *74*, 32.

(66) Weissleder, R.; Kelly, K.; Sun, E. Y.; Shtatland, T.; Josephson, L. Cell-specific targeting of nanoparticles by multivalent attachment of small molecules. *Nat. Biotechnol.* **2005**, *23*, 1418–1423.

(67) Kohler, N.; Sun, C.; Wang, J.; Zhang, M. Methotrexate-modified superparamagnetic nanoparticles and their intracellular uptake into human cancer cells. *Langmuir* **2005**, *21*, 8858–8864.

(68) Dodd, C. H.; Hsu, H. C.; Chu, W. J.; Yang, P.; Zhang, H. G.; Mountz, J. D., Jr.; Zinn, K.; Forder, J.; Josephson, L.; Weissleder, R.; Mountz, J. M.; Mountz, J. D. Normal T-cell response and in vivo magnetic resonance imaging of T cells loaded with HIV transactivator-peptide-derived superparamagnetic nanoparticles. *J. Immunol. Methods* **2001**, *256*, 89–105.

(69) Montet, X.; Montet-Abou, K.; Reynolds, F.; Weissleder, R.; Josephson, L. Nanoparticle imaging of integrins on tumor cells. *Neoplasia* **2006**, *8*, 214–222.

(70) Bullok, K. E.; Gammon, S. T.; Violini, S.; Prantner, A. M.; Villalobos, V. M.; Sharma, V.; Piwnic-Worms, D. Permeation peptide conjugates for in vivo molecular imaging applications. *Mol. Imaging* **2006**, *5*, 1–15.

(71) Schwalbe, M.; Jörke, C.; Buske, N.; Höffken, K.; Pachmann, K.; Clement, J. H. Selective reduction of the interaction of magnetic nanoparticles with leukocytes and tumor cells by human plasma. *J. Magn. Magn. Mater.* **2005**, *293*, 433–437.

(72) Zange, R.; Li, Y.; Kissel, T. Biocompatibility testing of ABA triblock copolymers consisting of poly(L-lactic-co-glycolic acid) A blocks attached to a central poly(ethylene oxide) B block under in vitro conditions using different L929 mouse fibroblasts cell culture models. *J. Controlled Release* **1998**, *56*, 249–258.

The MTT assay used here to assess *in vitro* cell viability is easy to setup and can be used with many different cell types. However, there are some drawbacks of this assay including relatively high standard deviations leading to high variability, short assay time of maximal 72 h, nonspecificity, and sensitivity of the cells to mechanical (abrasive) particle effects, which promote cell loss during rinsing.[73] Furthermore, the dark brown color of the magnetite nanoparticles, which changed the solution from a blue to a dark brown color, made photospectroscopic measurements more difficult. Possible alterations of the optical readings due to this background color were successfully corrected with a procedure described under Materials and Methods. Overall, these challenging technical details stemming from the MNPs would most likely result in the observed toxicities being exaggerated. Additional tests that might be useful in the future in addition to an MTT assay would be ones that measure apoptosis more specifically (e.g., with caspase and terminal transferase dUTP nick end labeling (TUNEL) assays), that measure the expression of specific biomarkers (e.g., Ki67 and cytokines such as interleukin-8 in endothelial cells[74]), and that measure membrane integrity (e.g., lactate dehydrogenase (LDH) and live/dead assays).[75]

In conclusion, MNPs coated with triblock copolymers containing PEO chains of 5 and 15 kDa are biocompatible as determined by a cell viability MTT assay. Furthermore, these MNPs at concentrations of up to 5 mg/mL do not disturb the growth of endothelial, epithelial, and tumor cells, as verified by confocal microscopy studies. Such MNPs can thus be tested *in vivo* for magnetic ocular drug targeting.

Acknowledgment. We thank Judy Drazba, Imaging Facility, Cleveland Clinic Foundation for assisting with the confocal microscopy and cell staining, and Dawn Smith at the University Hospitals of Cleveland and Diane Leigh, Lerner Research Institute, Cleveland Clinic Foundation for growing some of the needed cells. We appreciate the funding by DARPA and the Hertzel Foundation. We also thank Merck for support to F.M. with a summer student research fellowship.

Supporting Information Available: Movie of the entire set of 1 μm slices of confocal microscopy pictures. This material is available free of charge via the Internet at http://pubs.acs.org.

MP900083M

(73) Häfeli, U. O.; Pauer, G. J. In vitro and in vivo toxicity of magnetic microspheres. *J. Magn. Magn. Mater.* **1999**, *194*, 76–82.

(74) Peters, K.; Unger, R. E.; Kirkpatrick, C. J.; Gatti, A. M.; Monari, E. Effects of nano-scaled particles on endothelial cell function in vitro: Studies on viability, proliferation and inflammation. *J. Mater. Sci.: Mater. Med.* **2004**, *15*, 321–325.

(75) Häfeli, U. O.; Aue, J.; Damani, J. The Biocompatibility and Toxicity of Magnetic Particles. In *Magnetic Cell Separation*; Zborowski, M.; Chalmers, J. J., Eds.; Elsevier: Amsterdam, The Netherlands, 2007; pp 163−223.